Progress In Electromagnetics Research M, Vol. 113, 47–58, 2022

3D Printed Extended Lens as a Button Antenna for Off-Body Links at 60 GHz

Shakti S. Chauhan[1, *], Mahesh P. Abegaonkar[1], Ananjan Basu[1], and Djurdj Budimir[2]

Abstract—This paper presents a 3D printed extended hemispherical lens antenna for Body Centric Communications in 60 GHz band. The prototype consists of a 3D printed lens made of Polylactic Acid with three planar broadside patch antenna elements used as a source for the lens. The direction of the main beam antenna is switched by changing the excitation of source elements. The measured overlapping impedance bandwidth of the fabricated antenna is from 57.27 GHz to 60 GHz with reflection coefficient better than −10 dB. The main beam direction switches in broadside direction with 3 dB angular coverage from −29.2° to +30° by changing the radiating elements at 60 GHz. The measured gain is 15.28 dBi at 60 GHz. The beam switching capabilities and high gain with broadside radiation characteristics make the proposed antenna a suitable candidate for off-body links at 60 GHz. The effect of placing the antenna structure over the body is also studied in this paper. The body to off-body link measurement is successfully demonstrated with extended lens over the body and an open-ended waveguide as an external node.

1. INTRODUCTION

Body Area Network (BAN) is a wireless network of nodes which are inside the human body (implants), on the body (wearable) or around the body communicating with each other [1]. BAN found its implications in different fields like health, sports, and recreational purposes [2]. Such a network usually operates below 10 GHz. The bands below 10 GHz are already overcrowded by cellular and other wireless applications. So, it is better to move BANs in millimeter wave especially in ISM band at 60 GHz. The 60 GHz band is an unlicensed band with high atmospheric absorption [3], that leads to high attenuation which reduces its interference level [4]. The higher frequency operation at 60 GHz also allows smaller antenna size and higher data rates [3].

Antenna is the main component of the nodes for body centric communication. There are several antennas that have been reported at 60 GHz for on-body communication and off-body communication. For on-body links, a substrate integrated waveguide Yagi-Uda antenna [5, 6] and a printed Yagi-Uda antenna [7] with four single Yagi elements have been reported. Another Yagi antenna at 60 GHz that has been fabricated over a textile is presented in [8]. These Yagi-Uda antennas can be designed and optimised using optimising algorithms in terms of gain and side lobe levels [9, 10]. A wearable disc like antenna with an omnidirectional pattern for body links is discussed in [11]. A wide bandwidth Substrate Integrated Waveguide (SIW) horn antenna has been reported in [12]. A woodpile electromagnetic band gap (EBG) based antenna has been presented in [13]. There are very few works that have been reported for off-body links [14, 15] at 60 GHz band. In [14] and [15], a rectangular patch array is discussed. A rectangular loop with U-shaped patches is presented in [16] with the gain of 10 dBi. Most of the reported works for off-body links have demonstrated planar patch antenna with fixed beam directions.

Received 14 May 2022, Accepted 14 July 2022, Scheduled 8 September 2022
* Corresponding author: Shakti Singh Chauhan (shakti.uit@gmail.com).
[1] Centre for Applied Research in Electronics, IIT Delhi, Hauz Khas, India. [2] Wireless Communications Research Group, University of Westminster, London, UK.

For off-body links, a broadside pattern with high gain is desired. The antenna coverage of a high gain antenna is limited. The solution to this problem is a beam switching antenna with high gain.

The gain of the antenna can be improved by using extended hemispherical lens. In [17], a 3D printed extended hemispherical lens at 60 GHz has been discussed. Apart from that, the beam switching antennas using dielectric lens have been investigated for different applications [18–22]. However, none of the reported structures has been investigated under BAN application scenario. This paper proposes a new idea to implement a 3D printed extended lens antenna as a button antenna for establishing off-body links. The proposed structure is simple, low cost, and easy to fabricate because of 3D printing. Microstrip patch antennas are used to excite 3D printed lens and to test its performance, and extended lens is integrated over microstrip patch antennas on 5 mil substrates. The textile printed patch antenna can also be used instead of 5 mils substrate, and as in [23–25], textile antennas are designed for frequencies below 10 GHz. Textile antennas at 60 GHz frequency are also designed, but difference comes in terms of fabrication process for textile as compared to standard dielectric substrate-based antennas. The textile-based antennas at 60 GHz are more complex to fabricate (because of smaller antenna size at 60 GHz) and could have more loss at the desired frequency of operation, so standard dielectric substrate of thickness 5 mils is used in the proposed design. The main focus of the work is to implement beam switching using 3D printed lens over a thin dielectric substrate. Thus, the proposed structure that incorporates beam switching will improve the narrow beam coverage of high gain antennas. The size of designed antenna is small, so it can be easily integrated over the body. The antenna performance over the body is also analyzed using CST Simulation Software. The designed antenna is placed over a flat skin phantom of 5 mm thickness to analyse the effect of placing antenna structure over the body. The structure is proposed to be used as a button over the body surface to establish a link from the body toward the node which is externally located.

The paper is organised as follows. The lens theory and single element simulation is discussed in Section 2. In Section 3, beam switching is incorporated in the 3D printed lens antenna following Section 4, which discusses over the body antenna performance. Section 5 consists of measurement results of the proposed antenna and measured path gain of off-body link followed by conclusion.

2. SINGLE ELEMENT

This section explains the extended lens theory and design. This section includes simulation of extended lens integrated over a single rectangular patch.

2.1. Lens Theory

Dielectric lens at higher frequencies is designed using geometric optics. In [17], the reduced size lens is proposed for wireless chipset. The reduced extended hemispherical lens structure compromises with directivity [26], but for BAN applications, the small size of antenna is a priority. Therefore, a reduced size extended hemispherical lens is selected. The parametric view of reduced size extended lens is shown in Fig. 1(a). The diameter, d, of hemisphere is kept equal to $3\lambda_0$, where λ_0 is the free space wavelength. Thus, the diameter at 60 GHz is 15 mm. The hemispherical portion along with the extended length is used to approximate the elliptical lens profile as shown by the red curve in Fig. 1(a). Thus, the extended length, L, of the lens is calculated using equations [26, 27]:

$$L = b + c - d/2 \tag{1}$$

where '$a = d/2$' is half of the length of minor; 'b' is the half length of major axis; '$c = \sqrt{(b^2 - a^2)}$' is the distance from center to the foci of an approximated elliptical profile. For dielectric lens with an elliptical profile of substrate with refractive index n, equations are [27]:

$$\frac{\sqrt{(b^2 - a^2)}}{b} = \frac{1}{n} \tag{2}$$

$$c = \frac{b}{n} \tag{3}$$

From above equations, the extended length can be calculated depending on the refractive index of the lens material which in turn depends on the dielectric constant of the material. The material used for

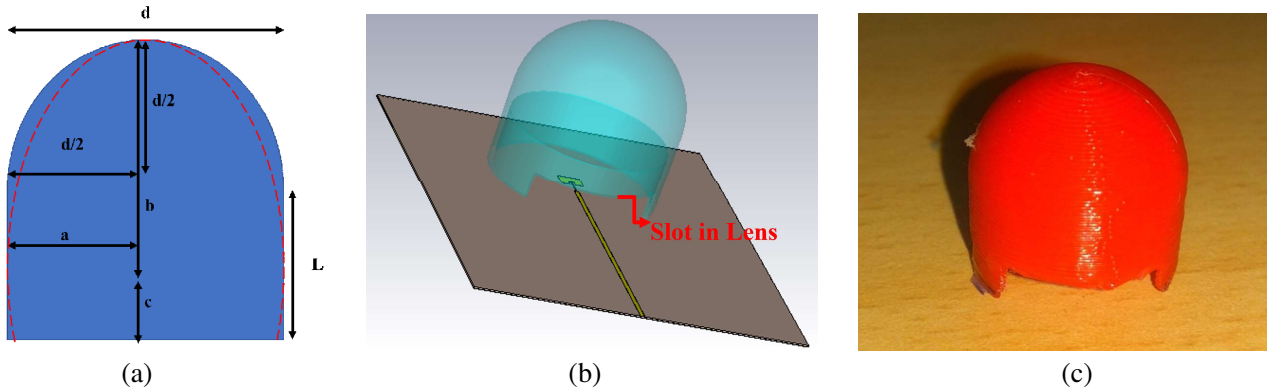

Figure 1. (a) Parametric view of extended lens with an elliptical profile; (b) Simulated structure of modified lens; (c) 3D printed Lens structure.

design of the lens structure is Polylactic Acid (PLA). The PLA is a thermoplastic that is used as the raw material for Fused Deposition Modelling (FDM) based 3D printing technology. The benefit of 3D printing is its cost effectiveness, and apparently any shape of lens can be fabricated using it.

2.2. Simulations

The dimension of the lens is calculated using Equations (1)–(3). As it is seen, the extended length of the lens depends upon dielectric constant of the material which is taken from 40 GHz–60 GHz in [28]. The diameter for the reduced lens is 15 mm ($3\lambda_0$), and the extension length of the lens is kept at 7.3 mm. Thus, the total length of the lens from the tip of the hemisphere to the foci of ellipse is around 14.8 mm. The small size of the lens structure makes it feasible to be used in BAN as a Button. The 3D printed lens is integrated over the microstrip patch antenna. The microstrip patch antenna is designed for a substrate of dielectric constant of 2.2 and thickness of 5 mils. The minimum feature size in the design is 100 microns. The dimension of the patch is 2 mm $\times$ 1.58 mm. The lens structure over the patch suffers internal reflections [26], which may lead into detuning of the reflection parameter of the designed antenna. So, in order to minimize these effects and to be used as a button, a cylindrical slot (an air cavity at the bottom of the lens structure) is made in the 3D printed lens as shown in Fig. 1(b). The structure simulated in CST simulation software is shown in Fig. 1(b), and the fabricated lens structure is shown in Fig. 1(c). The simulated reflection coefficient of the single element with lens integrated is shown in Fig. 2. It can be observed from Fig. 2 that the resonance frequency of the antenna is 59.12 GHz with simulated return loss of 25.70 dB at resonant frequency. The E-field distribution in Fig. 3 shows a comparison H-plane field of a microstrip patch antenna with and without lens integration. It can be clearly seen that the integration of lens over the patch will lead to the confinement of electromagnetic waves. The E-field confinement results in higher gain and a narrower beamwidth.

3. BEAM SWITCHING

The E-field confinement of the lens results in higher gain but narrower beamwidth. To overcome this, it is proposed to use beam switching for the extended hemispherical dielectric lens. In order to introduce beam shift, the patch is displaced off-center with respect to the axis of the lens along y-axis as shown in Fig. 4(a). The displacement of patch along the y-axis leads into the change of main beam direction and directivity [22]. In simulations, the patch is moved from the center to the distance of 5 mm in step size of 0.5 mm. It has been observed that the direction of main beam varies with respect to displacement of patch antenna as shown in Fig. 4(b). The main beam shifts from 0° to −26° with displacement of center patch to extreme most off-center position. It is seen from Fig. 4(c) that the side lobe level increases as the patch is moved away from center position. The side lobe level is maximum at the extreme off-center position of patch. The other main parameter which gets affected with the displacement of the patch is

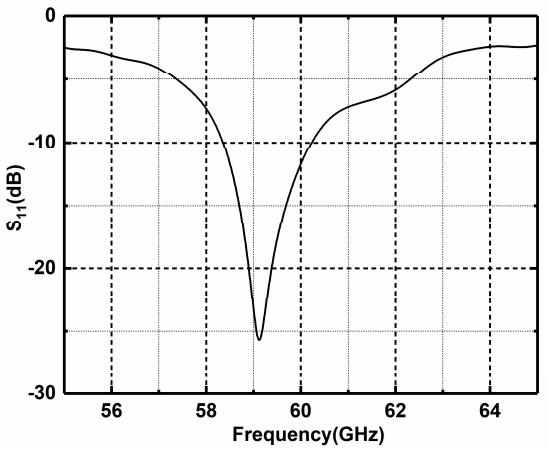

Figure 2. Simulated S-parameters of a single patch element with the lens integration over the patch.

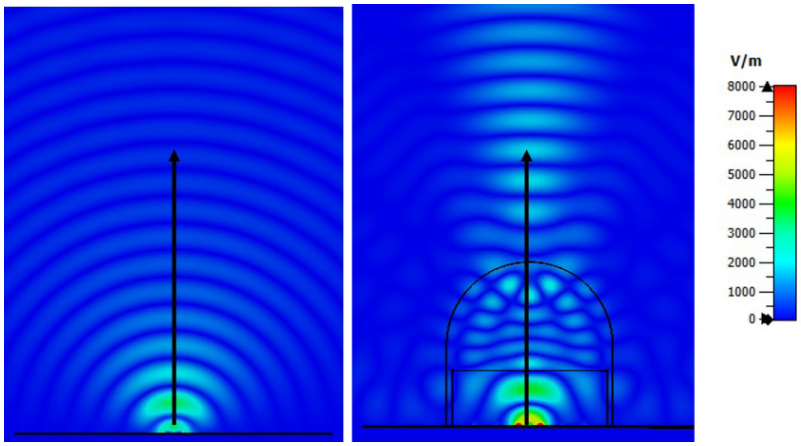

(a) (b)

Figure 3. Electric field distribution at 59 GHz in H-plane: (a) Patch without lens; (b) Patch with lens integration.

the gain of antenna, and the decrease in the gain with displacement is observed and shown in Fig. 4(d). Thus, it is seen that the off-center displacement leads to shifts in the main beam direction but also increase in the side lobe level and gain decrement.

The present work proposes an antenna with three patches which are located spatially in a line along y-axis. The edge-to-edge separation between them is kept 2 mm. The three patch antennas used to excite the lens are shown in Fig. 5(a). The complete structure with lens integrated over the microstrip patches is shown in Fig. 5(b). When center port is excited, the patch illuminates the lens, and the broadside beam of a rectangular patch gets confined after passing through the lens. It can be seen from Fig. 6(b) that the direction of main beam is 0° for the center patch. Thus, there is no tilting in main beam direction for center patch. When the excitation is switched from center patch to the left patch, the illumination source for the lens is off-center which results in beam tilting to the right of central axis of the lens as shown in Fig. 6(a). Similarly, Fig. 6(c) shows that when the excitation is switched to the right patch, the beam gets tilted to left of the central axis. Thus, a beam gets switched from left to right in H-plane with switching the excitation patches beneath the dielectric lens.

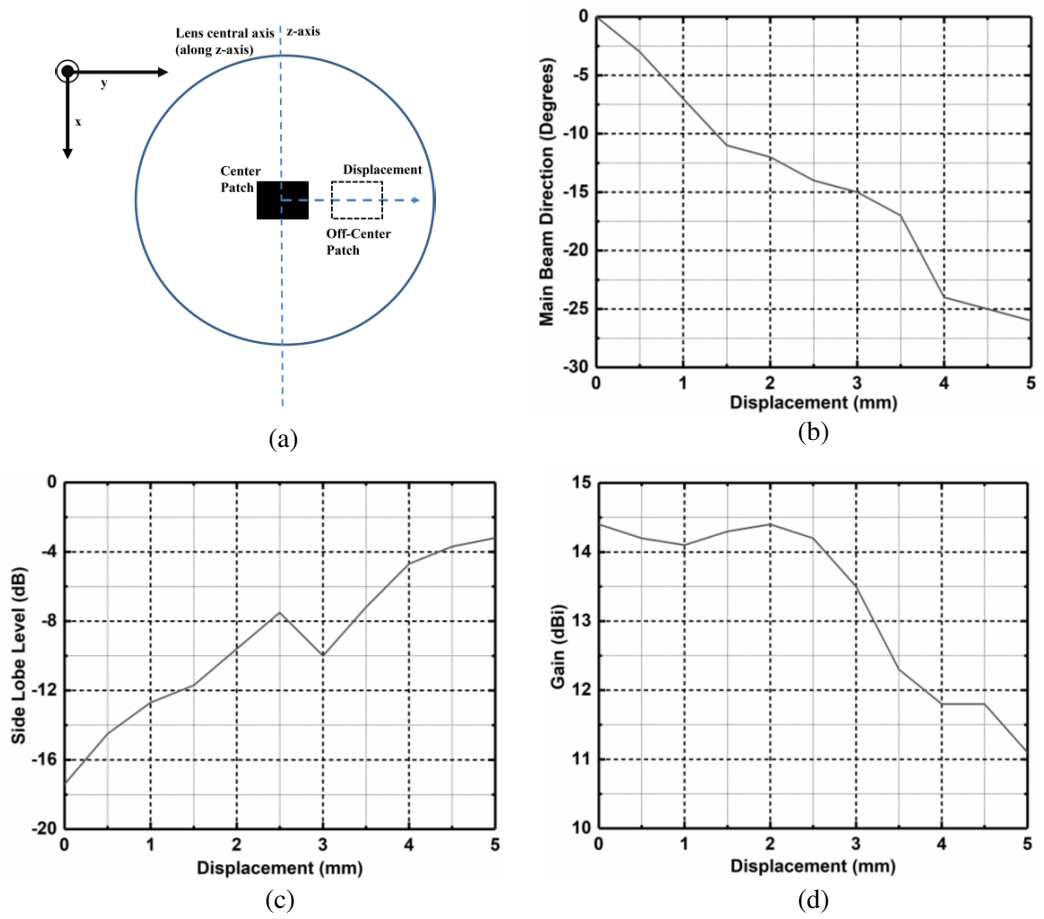

Figure 4. The variation of antenna parameters at 59 GHz with (a) displacement of patch from the central axis of the lens; (b) Main beam direction; (c) Side lobe level; (d) Gain.

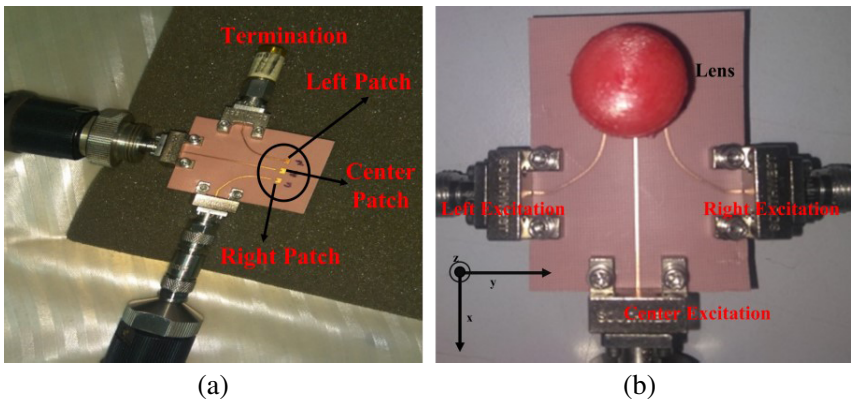

Figure 5. Fabricated structure for beam switching: (a) Without 3D printed lens; (b) With 3D printed lens.

4. OVER BODY ANTENNA PERFORMANCE

In order to study the real case scenario, the performance of antenna is simulated on the phantom. The antenna (patch dimensions: 2 mm ×1.58 mm and ground plane: 30 mm × 35 mm) is designed to work

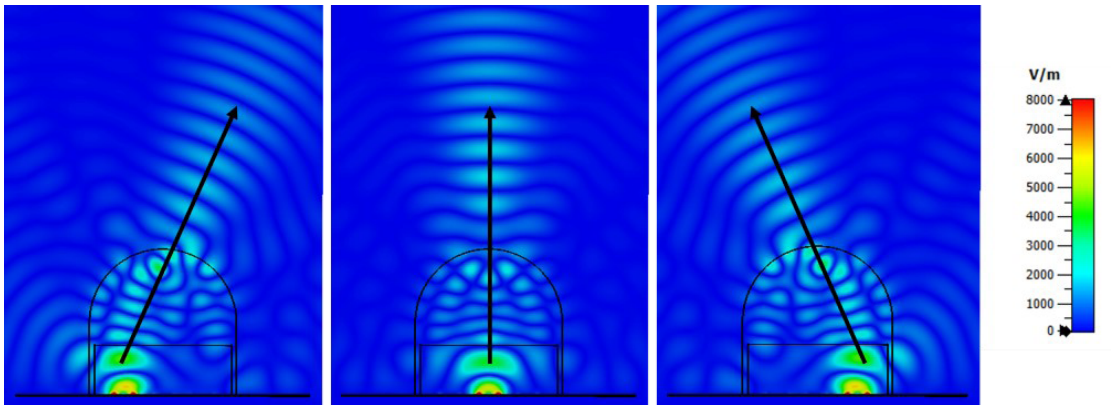

(a) (b) (c)

Figure 6. The E-field distribution at 59 GHz; (a) H-plane with left off-center patch for illumination; (b) H-plane with center patch for illumination; (c) H-plane with right off-center patch for illumination.

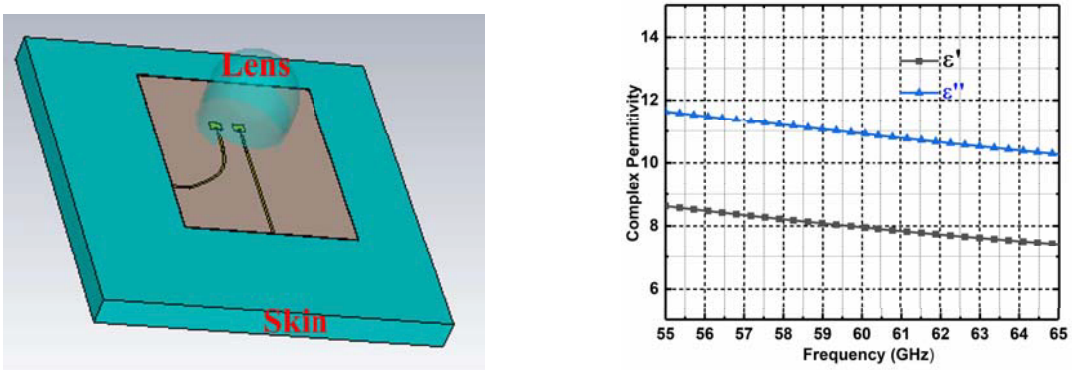

(a) (b)

Figure 7. (a) Antenna in close proximity of flat skin phantom; (b) Dispersive properties of the flat skin used in simulations.

as a button-shaped antenna and proposed to place the designed antenna structure over the chest for setting up off-body links. In order to replicate the human body effect, a flat skin phantom of size 60 mm $\times$ 60 mm is designed. Since the depth of electromagnetic wave at 60 GHz is about 0.5 mm [16], the thickness of the phantom is chosen as 5 mm. The skin has dispersive properties in terms of permittivity. The Debye's first order model is used to define the dispersive skin properties in the desired frequency range. The Debye's first order dispersion Equation (4), which is used to mimic human skin property, is given below [14]:

$$\varepsilon^* = \left(\varepsilon' - j\varepsilon''\right) = \left(\varepsilon_\infty + \frac{(\varepsilon_s - \varepsilon_\infty)}{(1 + j\omega\tau)}\right) \tag{4}$$

where ε^* is the complex permittivity; ε_s is the static permittivity; ε_∞ is the optical permittivity; ω is angular frequency; and τ is the relaxation time. The best fit values of Equation (4) are obtained in [14] and are given as $\varepsilon_s = 37.2$, $\varepsilon_\infty = 3.88$, and $\tau = 7.1 \times 10^{-12}$ s. The designed antenna over human flat skin phantom is shown in Fig. 7(a). In Fig. 7(b), the dispersive values of human skin are shown for the desired frequency range.

The complete antenna structure over the flat skin phantom is designed and simulated in CST simulation software. Only left and center patches are used as in simulation, and left and right patches are identical in terms of dimension, spacing from the center patch, and feed line. The antenna is simulated over the flat skin rectangular single layer phantom with a gap of 5 mm, and the effect on the antenna

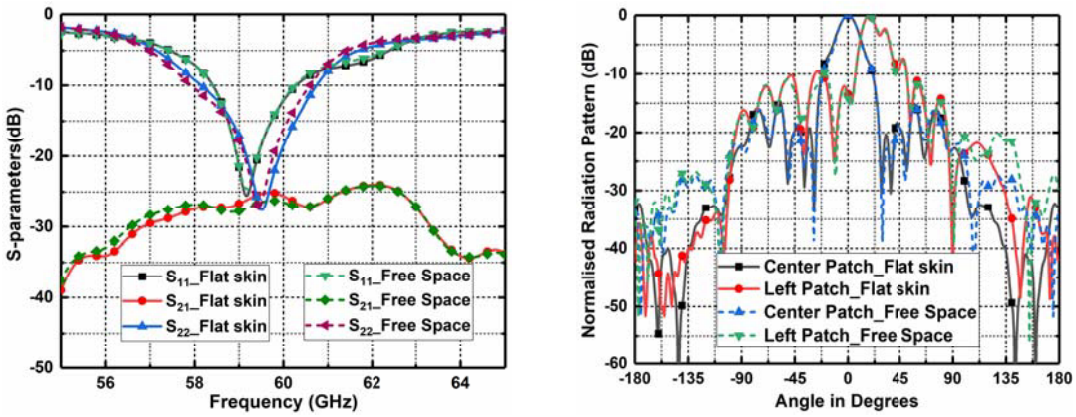

(a) (b)

Figure 8. Antenna characteristics in close proximity of flat skin: (a) S-parameters; (b) 2D Normalized radiation pattern in H-plane at 60 GHz. (Port 1: center patch and Port 2: left patch).

parameters is seen. The simulated S-parameters with and without the flat skin phantom are shown in Fig. 8(a). The reflection coefficients for only left and center patches are shown (with port 1 as center patch and port 2 as left patch excitation). It is clearly seen from the simulated results that placing the antenna over the phantom results in slight shift in resonance frequency of the designed antenna with respect to the free space reflection coefficients. The isolation between the antenna elements is also observed, and it is found that the isolation between different excitation patches is not much affected with placing the antenna over the flat skin phantom. Fig. 8(b) shows the normalised H-plane pattern in free space and over the phantom. It can be seen from the simulation results that the radiation pattern is also not affected much by the flat skin phantom. Therefore, it can be stated from above simulation results that the antenna's free space parameters are not affected much by placing it over the flat skin phantom. The result is evident as the antenna is radiating in the broadside direction away from the body, and hence it gets least affected by the placing over the human chest, where it is proposed to be used.

5. MEASUREMENT RESULTS

The antenna structure consists of a 3D printed lens fabricated using 3D printer and three patch elements fabricated using traditional lithography techniques on a 5 mils substrate of 2.2 dielectric constant. The fabricated antenna structure is shown in Fig. 5(b) and is characterized using Agilent PNA of up to 67 GHz.

5.1. Antenna Measurements

For s-parameter measurements, two ports are connected simultaneously with the feed line of two radiating patches while the third is connected to the 50 Ohm termination. The measured and simulated s-parameters of the fabricated structure are shown in Figs. 9(a)–(b). Port 1 is considered as for center feed excitation, while port 2 for left and port 3 for right feed excitation, respectively. The comparison between the simulated and measured s-parameters shows some deviation due to manual fabrication process, but they are still in good agreement. The measured 10 dB impedance bandwidth for the center patch is 56 GHz to 60 GHz, for the left patch is 56.25 GHz to 60 GHz, and for right patch is from 57.27 GHz to 60.44 GHz. The measured isolation between the center to left patch and left to right patch is shown in Fig. 9(b) in terms of s-parameters, and the isolation between rectangular patches is better than 25 dB. The radiation pattern of the antenna is measured using PNA. The normalized simulated and measured radiation patterns are compared, and it is observed that the main beams are pretty much similar. The measured beamwidth at 60 GHz for the center patch is 16.2° with the main beam direction

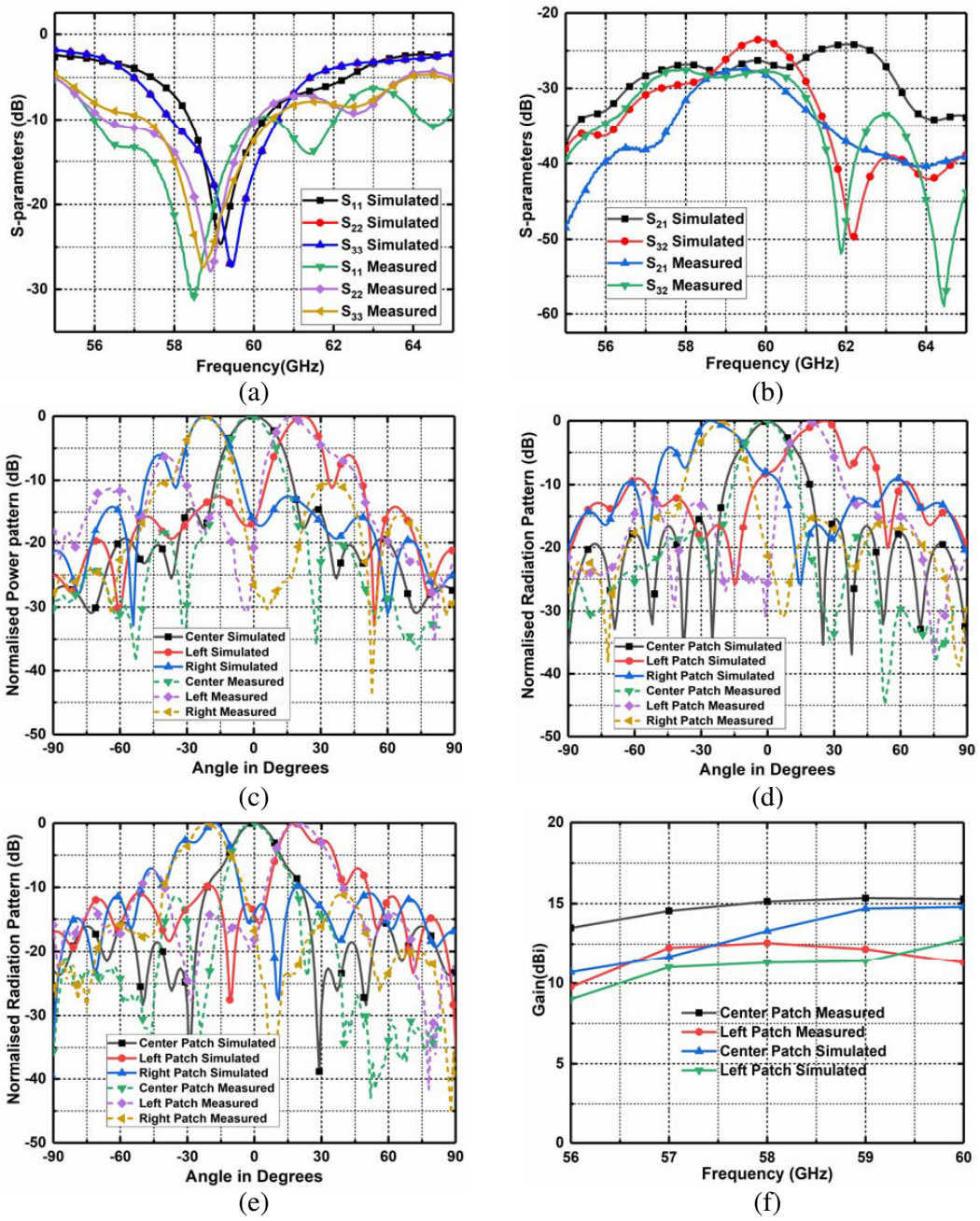

Figure 9. Antenna characteristics: (a) Reflection characteristics; (b) Isolation characteristics between antenna elements (in terms of *s*-parameter); (c) 2D pattern in *H*-plane at 56 GHz; (d) 2D pattern in *H*-plane at 58 GHz; (e) 2D pattern in *H*-plane at 60 GHz; (f) Gain.

at 0°, while the measured beam directions for the left patch and right patch are 17° (beam coverage: 11.3° to 30°) and −21° (beam coverage: −29.2° to −13.4°), respectively. In Fig. 9(f), the measured and simulated gains of 3D printed lens antenna are shown. The measured gains for center patch and left patch are around 15.28 dBi and 11.3 dBi, respectively at 60 GHz. From the gain curve, for center and left patches, it can be concluded that the gain for the off-center excitation sources is less than the gain of source which is axially aligned with the central axis of lens structure. So as the excitation moves away from the central axis of the lens, the beam gets tilted along with the reduction in gain comparative to the center patch.

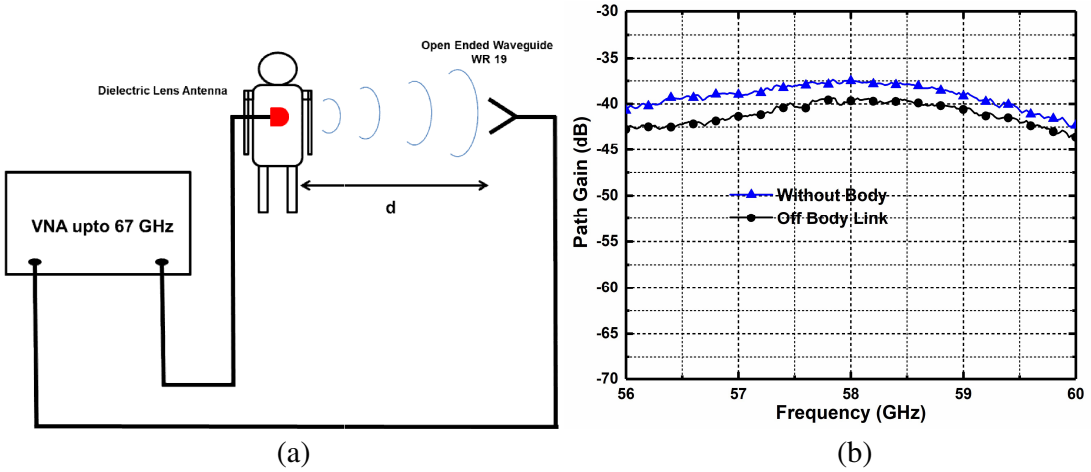

(a) (b)

Figure 10. (a) Measurement setup for path gain measurement; (b) Measured path gain for two different scenarios.

5.2. Path Gain Measurement

The antenna with a dielectric lens is measured for off-body links. The measurement setup is shown in Fig. 10(a). The high frequency cables are used to reduce the overall cable loss for the measurement of path gain. The setup also includes WR19 waveguides along with a pair of tripod stands, a fabricated lens antenna structure, and a PNA for S_{21} measurement in the desired frequency range. The frequency range selected for the measurement is 56 GHz to 60 GHz, since the antenna's impedance bandwidth lies in this range. The measured S_{21} includes cables losses, gain of the transmitting and receiving antennas, and the path loss. The loss factor due to cables is measured in thru state and is removed from the final path gain in two different scenarios. In the first scenario (without body), the designed antenna and WR19 (which is used as a standard antenna) both are fixed over tripod stand. In the second scenario

Table 1. Comparison table with state of the art antennas reported for BAN at 60 GHz.

Ref.	Antenna Structure	Propagation Type	Frequency Range (GHz)	Free Space Gain (dBi)	On Body Gain (dBi)
[7]	Printed Yagi Uda	On-Body	55–60	15	–
[8]	Wearable End fire Textile antenna	On-Body	57–64	9.2	11.9
[11]	Wearable Disc like antenna	On-Body	59.3–63.4	4.7	6.7
[12]	SIW Horn	On-Body	56.7–62.5	6.6	4.2
[13]	Woodpile EBG Based antenna: (a) Cylindrical; (b) Flat antenna	(a) On-Body (b) Off-Body	In V Band	–	–
[14]	Microstrip Patch Antenna Array on Thick Ground Plate	Off-Body	59–65	11.8	11.9
[15]	Wearable Textile: (a) microstrip Patch; (b) Patch Array	Off-Body	In V Band	(a) 4.2 (b) 8	(a) 3.5 (b) 7.8
[16]	Microstrip antenna with rectangular loop and U shaped Patches	On-Body/Body to off body	55–64.8	10.6	12
This Work	3D printed extended lens as a button antenna	Off-Body	57.20–60	15.38*	–

* Gain for center patch at 60 GHz

(off-body), the fabricated antenna structure is fixed over the human chest to replicate the scenario in which lens can be used as a button over the body. The open-ended waveguide remains fixed over the tripod stand which acts as off-body wireless node. The distance between two antennas is kept at 33 cm for both the scenarios. The two ports of PNA are used to excite the center patch of the lens antenna and open-ended waveguide, and S_{21} are measured between them. In Fig. 10(b), path gains for both cases are shown, and it is seen that they follow the same profile. The deviation in the path gain in both scenarios is around 2 dB at 58 GHz. The beam coverage for the center antenna is about 16.2°, but the beam switching capability in the designed antenna increases its angular coverage. The comparison table with other state of the art antennas for BAN at 60 GHz is shown in Table 1. From the comparison table, it can be concluded that the proposed extended lens antenna as a button can provide high gain, and the beam switching incorporated in it will give it an upper hand to the other reported structures for off-body links.

6. CONCLUSION

A 3D printed antenna with a beam switching capabilities is designed at 60 GHz. The 3D printed lens is low cost, easy to fabricate, and is used to increase the gain of the antenna which enables it to improve the path gain of off-body links. The designed beam switching structure provides simple, easy to fabricate, and low cost solution for off-body links at millimeter waves. The lens structure can be easily integrated as a button over the chest and used as a high gain broadside antenna for off-body links.

ACKNOWLEDGMENT

Mr. Shakti Singh Chauhan would like to thank Ministry of Electronics & IT, Government of India to provide support for PhD under Visvesvaraya PhD Scheme, and the UGC-UKIERI 2016 Scheme.

REFERENCES

1. Chavez-Santiago, R., et al., "Propagation models for IEEE 802.15.6 standardization of implant communication in body area networks," *IEEE Commun. Mag.*, Vol. 51, No. 8, 80–87, Aug. 2013.
2. Pellegrini, A., et al., "Antennas and propagation for body-centric wireless communications at millimeter-wave frequencies: A review [Wireless Corner]," *IEEE Antennas Propag. Mag.*, Vol. 55, No. 4, 262–287, Aug. 2013.
3. Park, C. and T. S. Rappaport, "Short-range wireless communications for next-generation networks: UWB, 60 GHz millimeter-wave WPAN, and ZigBee," *IEEE Wirel. Commun.*, Vol. 14, No. 4, 70–78, Aug. 2007.
4. Cotton, S. L., W. G. Scanlon, and P. S. Hall, "A simulated study of co-channel inter-BAN interference at 2.45 GHz and 60 GHz," *The 3rd European Wireless Technology Conference*, 61–64, 2010.
5. Wu, X. Y. and P. S. Hall, "Substrate integrated waveguide Yagi-Uda antenna," *Electron. Lett.*, Vol. 46, No. 23, 1541–1542, Nov. 2010.
6. Wu, X. Y., Y. Nechayev, and P. S. Hall, "Antenna design and channel measurements for on-body communications at 60 GHz," *2011 XXX URSI General Assembly and Scientific Symposium*, 1–4, 2011, doi: 10.1109/URSIGASS.2011.6123717.
7. Wu, X. Y., L. Akhoondzadeh-Asl, and P. S. Hall, "Printed Yagi-Uda array for on-body communication channels at 60 GHz," *Microw. Opt. Technol. Lett.*, Vol. 53, No. 12, 2728–2730, 2011.
8. Chahat, N., M. Zhadobov, L. L. Coq, and R. Sauleau, "Wearable endfire textile antenna for on-body communications at 60 GHz," *IEEE Antennas Wirel. Propag. Lett.*, Vol. 11, 799–802, 2012.
9. Recioui, A., "Application of a hybrid taguchi-genetic algorithm to the multiobjective design optimization of Yagi-Uda antennas," *Wireless Pers. Commun.*, Vol. 71, No. 2, 1403–1420, Jul. 2013, doi: 10.1007/s11277-012-0882-1.

10. Recioui, A. and Y. Grainat, "3D antenna array design using firefly optimization algorithm," *Algerian Journal of Signals and Systems*, Vol. 4, No. 2, 61–70, Dec. 2019.
11. Puskely, J., M. Pokorny, J. Lacik, and Z. Raida, "Wearable disc-like antenna for body-centric communications at 61 GHz," *IEEE Antennas Wirel. Propag. Lett.*, Vol. 14, 1490–1493, 2015.
12. Razafimahatratra, S., et al., "On-body propagation characterization with an H-plane Substrate Integrated Waveguide (SIW) horn antenna at 60 GHz," *2015 European Microwave Conference (EuMC)*, 211–214, 2015.
13. Brizzi, A., A. Pellegrini, L. Zhang, and Y. Hao, "Woodpile EBG-based antennas for body area networks at 60 GHz," *2012 4th International High Speed Intelligent Communication Forum*, 1–4, 2012.
14. Chahat, N., M. Zhadobov, L. L. Coq, S. I. Alekseev, and R. Sauleau, "Characterization of the interactions between a 60-GHz antenna and the human body in an off-body scenario," *IEEE Trans. Antennas Propag.*, Vol. 60, No. 12, 5958–5965, Dec. 2012.
15. Chahat, N., M. Zhadobov, and R. Sauleau, "Wearable textile patch antenna for BAN At 60 GHz," *2013 7th European Conference on Antennas and Propagation (EuCAP)*, 217–219, 2013.
16. Ur-Rehman, M., N. A. Malik, X. Yang, Q. H. Abbasi, Z. Zhang, and N. Zhao, "A low profile antenna for millimeter-wave body-centric applications," *IEEE Trans. Antennas Propag.*, Vol. 65, No. 12, 6329–6337, Dec. 2017.
17. Bisognin, A. et al., "3D printed plastic 60 GHz lens: Enabling innovative millimeter wave antenna solution and system," *2014 IEEE MTT-S International Microwave Symposium (IMS2014)*, 1–4, 2014.
18. Costa, J. R., E. B. Lima, and C. A. Fernandes, "Compact beam-steerable lens antenna for 60-GHz wireless communications," *IEEE Trans. Antennas Propag.*, Vol. 57, No. 10, 2926–2933, Oct. 2009.
19. Artemenko, A., A. Maltsev, R. Maslennikov, A. Sevastyanov, and V. Ssorin, "Beam steerable quartz integrated lens antenna for 60 GHz frequency band," *Proceedings of the 5th European Conference on Antennas and Propagation (EUCAP)*, 758–762, 2011.
20. Saleem, M. K., M. A. S. Alkanhal, A. F. Sheta, M. Abdel-Rahman, and M. Himdi, "Integrated lens antenna array with full azimuth plane beam scanning capability at 60 GHz," *Microw. Opt. Technol. Lett.*, Vol. 59, No. 1, 116–120, Jan. 2017.
21. Karttunen, A., J. Ala-Laurinaho, R. Sauleau, and A. V. Räisänen, "A study of extended hemispherical lenses for a high-gain beam-steering antenna," *Proceedings of the Fourth European Conference on Antennas and Propagation*, 1–5, 2010.
22. Filipovic, D. F., G. P. Gauthier, S. Raman, and G. M. Rebeiz, "Off-axis properties of silicon and quartz dielectric lens antennas," *IEEE Trans. Antennas Propag.*, Vol. 45, No. 5, 760–766, May 1997.
23. Osman, M. A. R., M. K. A. Rahim, N. A. Samsuri, H. A. M. Salim, and and M. F. Ali, "Embroidered fully textile wearable antenna for medical monitoring applications," *Progress In Electromagnetics Research*, Vol. 117, 321–337, 2011.
24. Soh, P. J., S. J. Boyes, G. Vandenbosch, Y. Huang, and and S. L. Ooi, "On-body characterization of dual-band all-textile PIFA," *Progress In Electromagnetics Research*, Vol. 129, 517–539, 2012.
25. Jais, M. I., M. F. B. Jamlos, M. Jusoh, T. Sabapathy, M. R. Kamarudin, R. B. Ahmad, A. A. Al-Hadi, E. I. B. Azmi, P. J. Soh, G. Vandenbosch, and N. L. Ishak, "A novel 2.45 GHz switchable beam textile antenna (Sbta) for outdoor wireless body area network (WBAN) applications," *Progress In Electromagnetics Research*, Vol. 138, 613–627, 2013.
26. Godi, G., R. Sauleau, and D. Thouroude, "Performance of reduced size substrate lens antennas for Millimeter-wave communications," *IEEE Trans. Antennas Propag.*, Vol. 53, No. 4, 1278–1286, Apr. 2005.
27. Filipovic, D. F., S. S. Gearhart, and G. M. Rebeiz, "Double-slot antennas on extended hemispherical and elliptical silicon dielectric lenses," *IEEE Trans. Microw. Theory Tech.*, Vol. 41, No. 10, 1738–1749, Oct. 1993.

28. Felício, J. M., C. A. Fernandes, and J. R. Costa, "Complex permittivity and anisotropy measurement of 3D-printed PLA at microwaves and millimeter-waves," *2016 22nd International Conference on Applied Electromagnetics and Communications (ICECOM)*, 1–6, 2016.